CNRS
Centre National de la Recherche Scientifique

INFN
Istituto Nazionale di Fisica Nucleare

VIRGO

Real-time simulation of interferometric gravitational wave detectors involving moving mirrors

Biplab BHAWAL

Groupe VIRGO, Laboratoire de l'Accélérateur Linéaire, CNRS-IN2P3, Batiment 208, Orsay Cedex, 91405, France.

VIR-NOT-LAL-1390-070
Issue: 1
Date : 09 December; 1996

VIRGO * A joint CNRS-INFN Project
Project Office: INFN-Sezione di Pisa * Via Livornese, 1291-56010 San Piero a Grado, Pisa Italia.
Secretariat: Telephone (39) 50 880 327 or 880 352 * FAX (39) 50 880 350 * e-mail virgo@pisa.infn.it

Abstract

A method of real-time dynamical simulation for laser interferometric gravitational wave detectors and various physical effects related to these are presented here. The method is based on a digital filtering approach and is applied with success for the dynamical simulation of 2-mirror cavities (both low and high finesse), 3-mirror coupled cavity and a full length power-recycled interferometer with mirrors having longitudinal motion. The details of the simulation procedure vary in different cases and sometimes new ways are developed to perform analytical calculations describing field evolution in various coupled or uncoupled cavities. Computer experiments performed with the fast simulation code for 3-mirror cavities also establish a rule for the appearance of resonance peaks in coupled cavities. Details related to the appearance of the dynamical peaks are also investigated and the related physical points are discussed. The final analytical representation used for the fast simulation of a full length power-recycled interferometer is analogous to a 2-mirror dynamical cavity with time-dependent reflectivities, when intra-cavity fields of the interferometer are expressed together in a state-vector representation. A detailed discussion establishes relationship among physical effects pertaining to field evolution in 2-mirror cavities and coupled cavities or the full interferometer. A proposal is made for a relatively easier *start-up* procedure for a dynamical power-recycled interferometer to bring it near to the operating condition from time zero.

1 Introduction

Gravitational wave detectors based on laser interferometry are currently being developed by various collaborating groups [1, 2, 3, 4]. Some common features to the long baseline facilities (as shown in Fig.1) are these: (a) To increase the storage time of light, Fabry Perot (FP) cavities to be used in the arms, (b) To maximise signal to noise ratio, the arm length difference to be so adjusted that the output port remains on the dark fringe, (c) To reduce the shot noise, high power laser to be used, in conjunction with power recycling technique[5], in which, at a dark fringe operation, the outgoing light is recycled back into the interferometer by putting a mirror in front of the source, thus enhancing the laser power, (d) To isolate mirrors from the seismic noise, all of the six mirrors to be suspended as pendulums.

The full interferometer is thus a system of coupled cavities. In addition to maintaining the dark fringe condition, all of these cavities are to be kept on resonance with the laser source. This is a difficult job since the suspended mirrors, by getting excited by the residual seismic noise, may oscillate around their equilibrium points at low frequency with an amplitude of some tens of wavelength.

All these features provide newer dimensions to the interferometry of the gravitational wave detectors. It should be noted that the physical effects related to dynamical single or coupled cavities and interferometers have been hardly discussed in the literature because of the simple reason that prior to the time the gravitational wave detectors got conceived, people could not even imagine designing such a system for some useful purpose.

A detailed investigation of these effects is necessary for a complete understanding of the operation of interferometric detectors. At this point of time, it is, therefore, extremely important to develop numerical simulation programmes that may predict the behaviour of the detector with sufficient level of accuracy. The need of this also arises in order to evaluate and optimize parameters of different components of the interferometer. We need to know how fields at various locations of the interferometer change as the mirrors move, so that we can utilize those informations to detect any variation in the required operating condition. An automatic length control system can then be developed based on these dynamical parameters.

It is straight-forward to write a simulation programme using exact equations of field evolution, but it takes too long computational time as compared to the real time to perform its calculation and so does not come to be of much/any use for either the control system or investigation of the

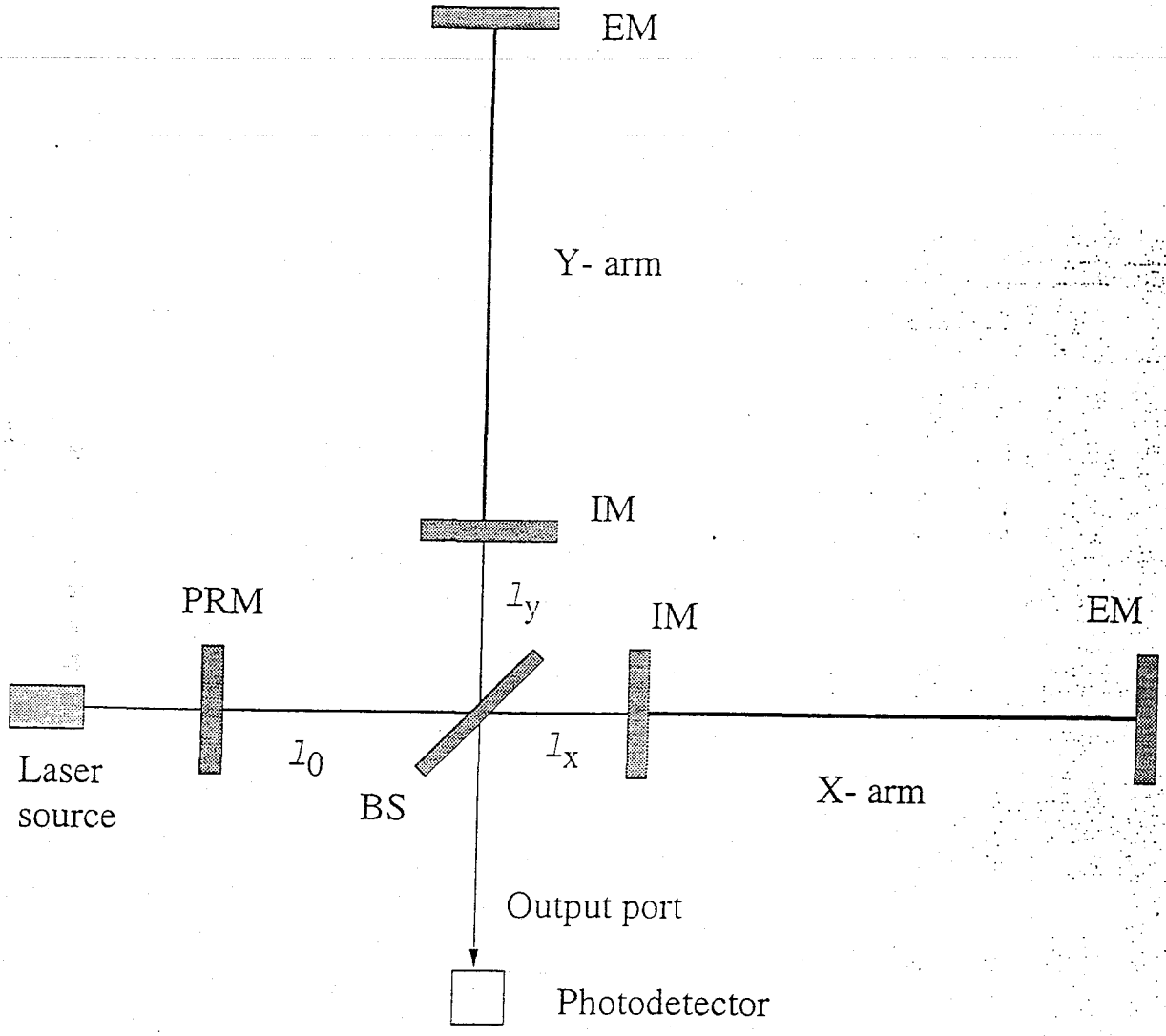

Figure 1: Configuration of a power recycled interferometer. BS - Beam Splitter EM - End Mirror, IM - Input Mirror, PRM - Power Recycling Mirror.

physical effects. This demands the requirement of fast simulation codes for a part or the whole of the interferometer which we can utilize for this purpose. If the behaviour of various servo responses can be properly ascertained, we can also compare performances of the real interferometer with the one running in computer (provided the latter is fast enough) and initiate proper action if anything goes wrong during operation. Such a complete simulation incorporating both signal generated by moving mirrors in a high finesse 2-mirror cavity and the response of the servo control system has been reported by the LIGO team[6].

With these objectives in mind, in this paper, I develop a method of dynamical simulation for a power-recycled interferometer, which is able to perform real-time calculations for various levels of accuracy. The method is based on a digital filtering approach and a number of important physical points understood by a step-by-step investigation process. This investigation finally establishes relationship among characteristics of dynamical field evolution in a long-baseline interferometer with those in 2-mirror and 3-mirror coupled cavities. Therefore, in sections 2, 3, 4, I introduce various aspects of this method and discuss the characteristics of dynamical response in low finesse 2-mirror cavity, high finesse 2-mirror cavity and a 3-mirror coupled cavity respectively. The special features of coupling between recycling cavity and arm cavity are discussed in sec. 5 with the help of the results obtained by performing computer experiments using the fast code developed for 3-mirror coupled cavity. Finally, in sec. 6, I use all the understandings arrived at through this step-by-step process along with the techniques developed thereby to write the fast numerical code for power-recycled interferometer. The physical effects related to the coupling of fields in-between two arm cavities of an interferometer are also discussed and on the basis of these points, in the same section, I propose a relatively easier method for solving the *start-up* problem of such interferometers, i.e., to bring all the coupled cavities near to the resonant condition starting from time zero. Section 7 summarizes important conclusions on the physical effects in a dynamical power-recycled interferometer as well as considerations about the computational speed of the codes developed.

2 Fast simulation of low finesse 2-mirror cavities : Digital filtering approach based on *Perturbation method*

In this section, I study the simplest case of simulation, i.e., that of a 2-mirror cavity of low finesse. Such a cavity of finesse about 50 will be used in the arms of the VIRGO interferometer. We may note in advance that a direct analogy can be established between the response of a power-recycled interferometer and that of a 2-mirror cavity under general dynamical conditions, as will be shown in sec.6. The dynamical response may show low or high finesse characteristics depending on the operating condition of a light beam. Results of the investigation in this section are, therefore, very important and will be applied in writing the simulation programme of the whole interferometer in sec.6.

An analogy is established here between a digital filter and the linear response of a cavity towards small motion of mirrors. A fast simulation procedure based on this is developed thereafter [7]. The analytical calculation presented here for the response of a low finesse cavity is based on the perturbative technique. I investigate how well such a perturbative calculation can describe the evolution of fields when used in the fast dynamical simulation procedure based on digital filtering approach (DFA). The numerical results and comparison with other methods are also presented.

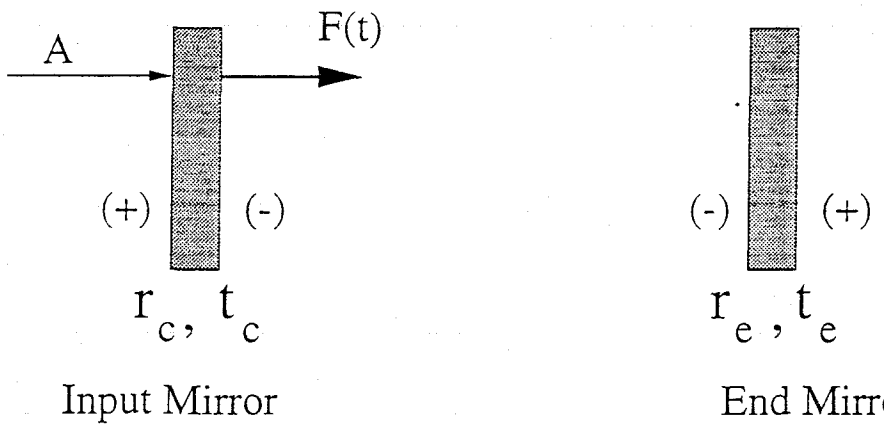

Figure 2: Notation for a 2-mirror cavity; r_c (r_e) and t_c (t_e) are amplitude reflectivity and transmittivity respectively for the input (end) mirror. The sign (+) or (−) indicates the phase acquired on reflection from that side of the mirror.

2.1 Cavity linearized equation

Let us first write down the exact equation for the intra-cavity field, F based on the notation of Fig.2 by taking the laser source to be the reference point for the motion of the mirrors:

$$F(t) = t_c A \exp j[\frac{2\pi}{\lambda} x_c(t)] + r_c r_e \exp j[\theta(t-\tau/2)] F(t-\tau), \quad (1)$$

where $\tau = 2L/c = 2 \times 10^{-5}$ sec. is the round-trip time for VIRGO 3-Km cavities and λ is the wavelength of the laser light, 1.064μmeter: t_c is the amplitude transmittivity of the input mirror, whereas r_c and r_e are the amplitude-reflectivities of the input and end mirror respectively. The quantity, $\theta(t)$ represents round-trip phase offset in the cavity at any time t:

$$\theta(t-\tau/2) = \phi + \frac{2\pi}{\lambda} 2x(t-\tau/2), \quad (2)$$

where ϕ is the initial (comnstant) round-trip phase offset and $x(t-\tau/2)$ is variation in the length of the cavity as experienced by the light at time t due to the movement of the mirrors:

$$2x(t-\tau/2) = -x_c(t-\tau) + 2x_e(t-\tau/2) - x_c(t), \quad (3)$$

where $x_c(t)$ and $x_e(t)$ are displacements of the input and the end mirror respectively.

If we assume that both the variation. $x(t)$ of the length, L of the cavity and the frequency of such variation are small enough, we can reasonably predict that the field amplitudes will also vary slowly around some stationary point (an elaborate and nicer treatment can be found in Ref.[8]). The Eq.(1) can, therefore, be written in the following form for small x :

$$F(t) = t_1 A \exp j[\frac{2\pi}{\lambda} x_c(t)] + R[1 + j\frac{2\pi}{\lambda} 2x(t-\frac{\tau}{2})] F(t-\tau), \quad (4)$$

where

$$R = r_c r_e \exp j[\phi]. \quad (5)$$

Note that we make a simplifying assumption that the input light, A is constant. The stationary point of the intracavity field can thus be written from the zeroth order equation:

$$F_0 = \frac{t_c A}{1-R}. \quad (6)$$

which just represents the quasi-static field, i.e., when mirrors do not move at all or moves so slowly that it does not affect anything for a long time. The variation of the intra-cavity light from this can be obtained from the first order equation:

$$\delta F(t) = R[\delta F(t-\tau) + j\frac{4\pi}{\lambda}F_0 x(t-\frac{\tau}{2})]. \tag{7}$$

This leads to the following transfer function for the cavity in the s-domain of the Laplace transformation:

$$H_c(s) = \frac{\delta F(s)}{x(s)} = jPF_0\frac{\exp(-\frac{\tau}{2}s)}{1-R\exp(-\tau s)}x(s), \tag{8}$$

where

$$P = (\frac{2\pi}{\lambda})R. \tag{9}$$

The Eq.(8), as such, is not of much use for the time domain simulation, since we need to know $x(t)$ in the full time domain ($t \to +\infty$) for the calculation of $\delta B(s)$. However, as is discussed in the next subsection, the technique of digital filtering can be appropriately applied to take advantage of the linear equation (7) with the objective of developing a fast computational method for the variation in the intracavity light.

2.2 Cavity as a digital filter

A number of standard texts [9, 10] on digital filters are available. However, it is worthwhile introducing a few important concepts here to understand the domain of validity of the analogy between a cavity and a digital filter, which I am going to describe.

Let us consider a transfer function of the following form corresponding to the input, X and output, Y in the s-domain :

$$H(s) = \frac{Y(s)}{X(s)} = \frac{\sum_{k=0}^{K} C_k \exp(-ks\Delta)}{1-\sum_{m=1}^{M} D_m \exp(-ms\Delta)}, \tag{10}$$

where k and m are integers and Δ is some fixed time interval.

The correspondence between this transfer function and its own discrete form in the Z-transform domain can be established by a conformal transformation, $z = \exp(s\Delta)$:

$$\bar{H}(n) = \frac{\bar{Y}(n)}{\bar{X}(n)} = \frac{\sum_{k=0}^{K} C_k z^{-k}}{1-\sum_{m=1}^{M} D_m z^{-m}}. \tag{11}$$

where n represents the sampled points with a time period, Δ.

So, one can now arrive at the following equation describing the output function in its discrete form :

$$\bar{Y}(n) = \sum_{k=0}^{K} C_k \bar{X}(n-k) + \sum_{m=2}^{M} D_m \bar{Y}(n-m). \tag{12}$$

This is known as the *infinite impulse response* (IIR) filter which is actually a series of feedback loops as is obvious from the equation above.

Let us now look back at Eq.(7) and compare it with Eqs.(11,12). We can easily see that Eq.(7), as such, can provide only two nonzero coefficients ($C_1 = PB_0$ and $D_2 = re^{j\phi}$) for the evaluation of

the output,i.e., the variation in the intracavity light, δB in the discrete time domain with a sampling period of $\tau/2$. However, if we wish, we can always increase the number of the coefficients, C_k simply by explicitly evolving the recursive relation, Eq.(7), in N steps for time $N\tau$. In optical language, this is equivalent to tracing the path of the light for N number of bounces on the moving end-mirror.

It should be noted that such a procedure, however, does not increase the number of nonzero D_m coefficients and, in fact, reduces the numerical importance of the only available coefficient (which is D_m for $m = 2n$ at any stage, n) at every step of this evolution by a factor R. So, if we are able to take a sufficiently large value of N, we can reasonably neglect the contribution of previous outputs in the present value of the output in a low finesse cavity. Such a filter which does not receive any input in the form of a feedback is called *finite impulse response* (FIR) filter and for such filters, the coefficients, C_k represent the unity impulse response of the filter. It should be noted that by going through this step, the concept of the cavity as a filter got converted from an IIR one to a FIR one.

In the context of a two-mirror cavity, we can thus write down the following equation for the intra-cavity light directly from Eq.(7):

$$F(t + N\tau) = \frac{t_1 A \exp j[x_c(t)]}{1 - R}(1 + jP \ \text{Sum}) \tag{13}$$

where

$$\text{Sum} = \sum_{n=1}^{N} R^{N-n} x(t + (n - \frac{1}{2})\tau). \tag{14}$$

The structure of the correction term shows that it is nothing but the time-convolution of the input, $x(n)$ with the unity-impulse response-function represented by the coefficients,

$$C_k = jPF_0R^{k-1}, \quad \text{where} \quad k = 1, 2, 3, \ldots \tag{15}$$

Before we go to the next section we should keep in mind that the usefulness of the analysis presented here depends strongly on the validity of the assumption that the mirror movement is very slow which enables us to use the linear equation for the cavity. So, the validity of the analysis depends on how we make a suitable choice for the number of bounces, N. The value of N is to be ascertained numerically in the next subsection by taking error considerations into account.

2.3 Simulation and results

The numerical investigation shows that the phase factor which depends on $x_c(t)$ in Eq.(13) has almost no influence on the evolution of fields in a low finesse cavity (note that it will not be so in the next section, when we discuss about high finesse cavities). So, while developing the following simulation technique, we can safely ignore this factor. This also means that for a low finesse cavity, it does not matter whether we take the laser source or the input mirror to be our reference point of mirror motion, provided the speed of the input mirror is of the order of 1 μm/sec or less than that.

The procedure of the numerical simulation is as follows:

- **step 1**: Time is sliced into equal intervals of width $\Delta = N\tau$, so that any time $t_i = iN\tau$, where i is an integer.

- **step 2**: The phase, ϕ is fixed to the following value during any time interval (t_i, t_{i+1})

$$\phi_i = \phi_0 + \frac{4\pi}{\lambda} x(i\Delta). \tag{16}$$

where ϕ_0 is a small initial phase offset at time $t = 0$.

•**step 3**: During the time interval (t_i, t_{i+1}), the rate of change of the cavity length is also assumed to be constant

$$w_i = \frac{x_{i+1} - x_i}{N\tau} \tag{17}$$

This is a valid assumption, as long as the frequency of mirror oscillation is small and we choose a reasonable value of N. For example, for a frequency of, say, 200mHz, we can reasonably talk about a value of N up to, say, 200 without making much error.

•**step 4**: The assumption in step 3 enables us to arrive at a very simple expression for the convolution-sum in Eq.(13). This sum now turns out to be an *arithmetico-geometric* series which can be easily converted into its compact form [11]. So,

$$\text{Sum} = \frac{(N - \frac{1}{2}) - (N + \frac{1}{2}) r_e r_c \exp j[\phi_i]}{(1 - r_c r_e \exp j[\phi_i])^2} w_i \tau + \mathcal{O}(R^N) \tag{18}$$

The $\mathcal{O}(R^N)$ terms can be neglected for sufficiently large values of N.

•**step 5**: Substituting $i \leftarrow i + 1$, the same procedure is repeated again,i.e., the values of ϕ_i and w_i are changed in the next step and B_{i+1} is calculated.

As one can see, this method makes a slope-by-slope approximation of the actual mirror movement, where each slope (velocity, w_i) lasts for a short time. The span of this short time (represented by N) can be decided by numerical investigation of the error level introduced by slope-by-slope approximation.

The above method based on a digital filtering approach (DFA) can now be compared with other methods[12] of simulation which have been tried in order to get a fast simulation of low-finesse cavity: (a) *the sequential method* (SM), which computes the intracavity beam at each round-trip and so is accurate but very slow, (b) *the quasi-static method* (QSM) that just computes a stationary value from the cavity Airy function (Eq.6) for the intracavity light on the assumption of constancy of all quantites over a sufficiently long time and thus its error is independent of the time-step used in the computation, (c) *the differential equation method* (DEM) [12] which under the assumption of constancy of x (and thus of the phase offset) over an interval $\Delta = N\tau$, solves the cavity differential equation in that interval, sets the initial condition for the next step with that solution, changes the phase by another step and solves the differential equation again. As a result, for smaller values of N, the DEM approaches the accurate SM and for higher values of N, it approaches the QSM.

An important difference between the DEM method and the present method is that while the former makes a step-by-step approximation (i.e. x is constant over the interval Δ) for the mirror displacement, $x(t)$, the present method takes a slope-by-slope approach (i.e., x changes with constant velocity during Δ) for the same. As a result, a comparison between either DEM or QSM and the present method can only be made for small values of N. For large values of N, such a comparison is meaningless since, in that case, only in the limit $w \to 0$, the present method can be expected to be similar to either QSM or DEM.

The simulation program as described in the last section is run for two values of mirror velocity (which, for the sake of simplicity, has been assumed to be constant throughout the time of simulation), 1μm/sec and 0.5μm/sec. The values of r_c and r_e are chosen to be 94.0% and 99.99% respectively, which corresponds to a finesse of approximately 50[2]. A power-loss of 10 ppm has been considered for both mirrors.

A typical resonance curve generated by the exact SM method for such a cavity with $w = 1\mu$m/sec is shown in Fig.3. The resonance curve generated by either QSM or DFA method under similar

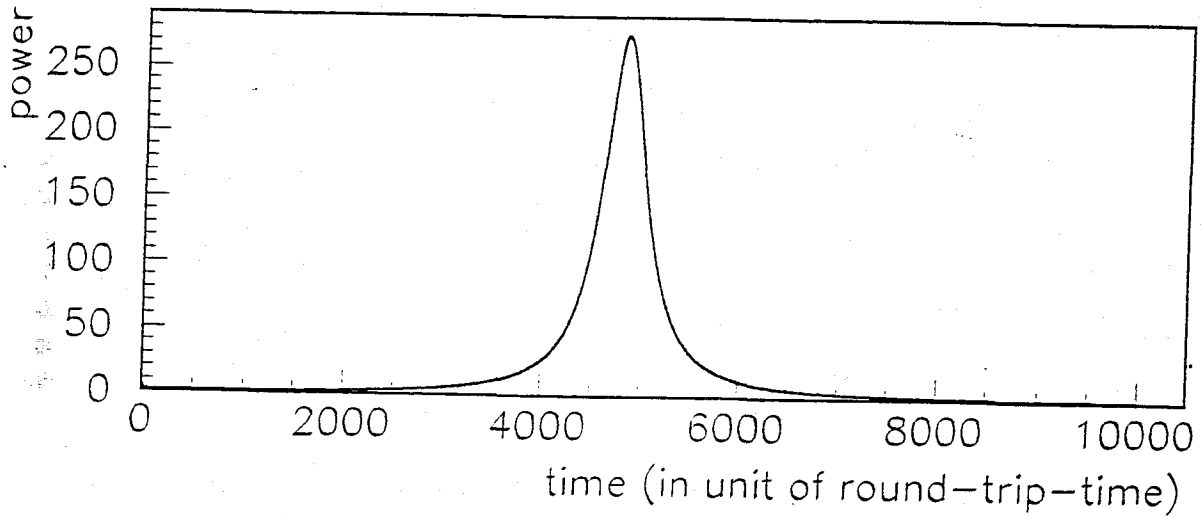

Figure 3: A typical resonance curve for a low finesse cavity that can be drawn by using SM or QSM or DEM or DFA method (with reasonable values of N in the last two cases), while the cavity length changes at a rate $w = 1\mu$m/sec. Input power, $|A|^2$ is assumed to be one unit. Note that the resolution of the plot can not make difference among curves obtained from these methods. The error levels of QSM and DFA are shown in the next figure.

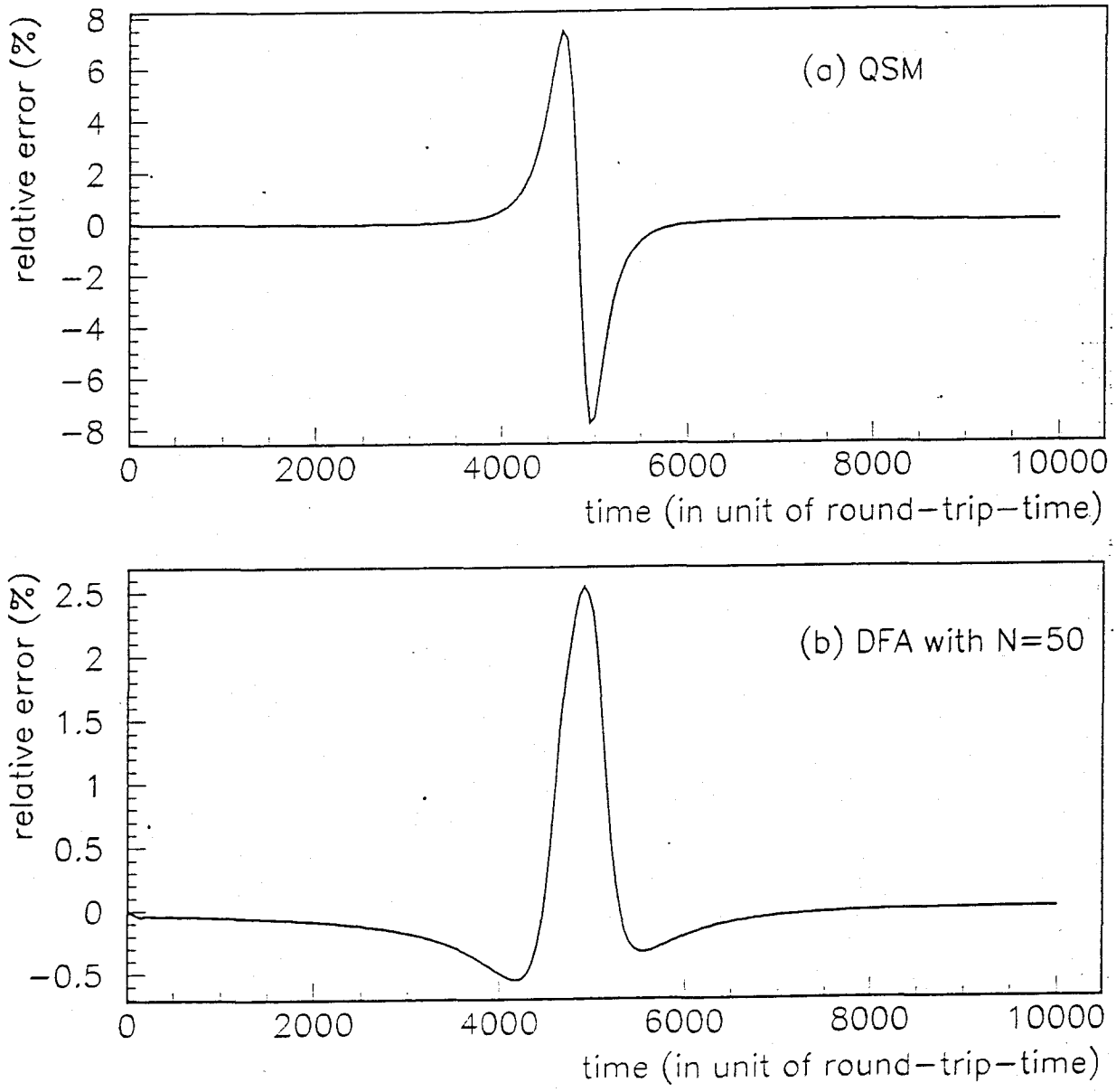

Figure 4: Relative error (%) of (a) QSM and (b) DFA based on perturbative calculation as compared to the exact SM in computing the resonance curve of Fig.3. Note that the error level of QSM is independent of the choice of the number of steps, N (provided N is not so large that the sampling of values becomes meaningless).

conditions looks to be similar to the above curve, but any of these methods actually makes some error (wrt the SM), which remains to be invisible by the resolution of the plot.

The 'relative error' made by either QSM or DFA with respect to (wrt) the accurate SM method in drawing the same resonance curve is plotted in Fig.4. The *relative error of some method Y wrt some other method X*, is defined as follows:

$$\text{Relative error}(\%) \;=\; \frac{\text{value predicted by Y} - \text{value given by X}}{\text{value given by X}} \times 100. \qquad (19)$$

The nature of the error curve for DFA as shown in Fig.4(b) is more or less similar for various values of N and w, but is quite different from those for either QSM (Fig.4a) or DEM. The error curves generated by QSM and DEM are similar looking, but the level of error is less in DEM as compared to QSM[12]).

The maximum values of the error curves of the DFA as a function of N have been plotted in Fig.5. One can see that the simulation performs quite satisfactorily even for large values of N (= say 60 for $w = 1\mu$m/sec or say 100 for $w = 0.5\mu$m/sec, if we take an arbitrary value of about 4% to be an upper limit). I neglected $\mathcal{O}(r^N)$ terms in Eq.(18) for simulation and thus for sufficiently low value of N, the maximum value of error increases again, as can be seen in Fig.5.

The relative error increases not only for higher values of N and/or mirror-velocity, but also for higher values of the cavity finesse. The finesse of a cavity can as well be expressed by the product of the amplitude-reflectivities of the two mirrors. Since we always keep the value of r_e equal to a constant, 99.99%, from now onwards I always refer to the finesse of a cavity in terms of the reflectivity of the input mirror, r_c.

Now we fix $N = 50$ and tabulate the maximum values of error curves generated by DFA for increasing values of r_c in Table 1. As we can see, the error increases too fast just after crossing the value $r_c = 0.975$. A validity domain for this method based on perturbative calculations may be ascertained in terms of an upper limit of about 0.975 on r_c for a mirror velocity of ≤ 1 μmeter/sec; This limit, however, depends on what trade-off one would like to make between computational speed and error in its application and should be mentioned in that spirit. But whatever be the trade-off, the perturbative calculation of cavity response is certainly not applicable in the digital filtering approach of fast simulation for a value of finesse corresponding to $r_c \geq 0.99$. So, we need to replace the perturbative calculation by some other method in the framework of the digital filtering approach of fast simulation when we intend to apply the same to high finesse cavities.

From now onwards, we refer to cavities with $r_c \leq 0.975$ as *low finesse cavities* and those with $r_c \geq 0.985$ as *high finesse cavities*. The cavities with $0.975 < r_c < 0.985$ correspond to the intermediate range for which a perturbative approach of simulation leads to too much of error for high values of mirror velocities (i.e.≈ 1 μm/sec.), but, on the other hand, for which the high-finesse characteristics of the cavity response (as I discuss in the next section) are not so prominent. In any case, the fast simulation methods to be developed in the next section for high finesse cavities can always be applied to lower finesse cavities. I am making this division in the range of finesse just to make a clear-cut distinction between the high finesse and low finesse characteristics, which 1allows us a convenient basis of our discussion.